RADIOSITY–CALCULATIONS FOR ROTATIONAL SURFACES

Helmut Mastal **Robert F. Tobler** **Werner Purgathofer**

Institute of Computer Graphics, Vienna University of Technology
Karlsplatz 13/186/2, A-1040 Vienna, AUSTRIA
mastal@edvz.tuwien.ac.at, {rft,wp}@cg.tuwien.ac.at

ABSTRACT

Rotational Surfaces are very important for photorealistic representations of plants and other natural phenomena. In this paper radiosity calculations for rotational surfaces are presented that handle surfaces as whole objects rather than approximating them by large numbers of plane patches. Mathematical expressions are given for the radiance of cylinders, cones and spheres that are ideal Lambertian reflectors. Although there exists no complete radiosity algorithm which uses the formulae for cylinders, cones and spheres at the moment, it can be estimated that the number of objects of a global illumination scene as well as the number of interactions could be reduced dramatically. Therefore it should be possible to render more complex scenes with plants, like forests, in reasonable time.

Keywords: radiosity, rotational surfaces, natural phenomena

1 INTRODUCTION

Radiosity methods in the past originated from the theory of radiative heat transfer that was applied to computer graphics by Goral et al. [Goral 84]. The primary assumption of radiative heat transfer was that every object of a scene consists of a limited number of plane patches and these patches exchange energy to each other. Radiosity theory was developed further by Cohen et al. to the hemi-cube technique [Cohe 85] and to substructuring [Cohe 86].

The plane patch assumption has been still propagated to most of the radiosity methods presented up to now. Galerkin radiosity [Zatz 93] is an exception, it is not really limited to plane patches. Even hierarchical radiosity methods [Hanr 91] and Monte Carlo methods [Shir 90] assume the lower level elements of complex surfaces to be plane polygons.

In nature, however, plane surfaces are not very common. For the photorealistic representation of outdoor scenes with plants and other natural objects the direct rendering of curved surfaces like cylinders or cones in contrast would be very desirable. In [Gerv 96] whole objects are used for the representation of plants with an algorithm based on ray-tracing. Also [Stam 97] claims to handle general curved surfaces with the bounded radiosity method, especially in the case where no subdivision of an object is required.

But with most radiosity based global illumination methods curved surfaces have to be approximated by a large number of plane patches to give an accurate picture of the curved object. For a sphere to achieve a good approximation one has to divide the polar angle into 20 zones and the azimuthal angle into 24 zones (giving approximately squares at 53^0 latitude). So 480 patches are obtained from one object. Although this is an extreme example, a curved surface normally will be replaced by 10 to 100 plane patches. Since an outdoor scene of natural objects can consist of 10^5 objects or more, the number of patches for radiosity calculations will be about 10^7, the number of energy interactions will be about 10^{14}.

The aim of this paper is to reduce the number of elements and of interactions for scenes of natural phenomena. Therefore curved surfaces will be considered as whole objects for the purpose of calculating the ideal diffuse reflection rather than approximating them by plane patches.

Prusinkiewicz and Lindenmayer [Prus 90] distinguish between two kinds of shapes that build up

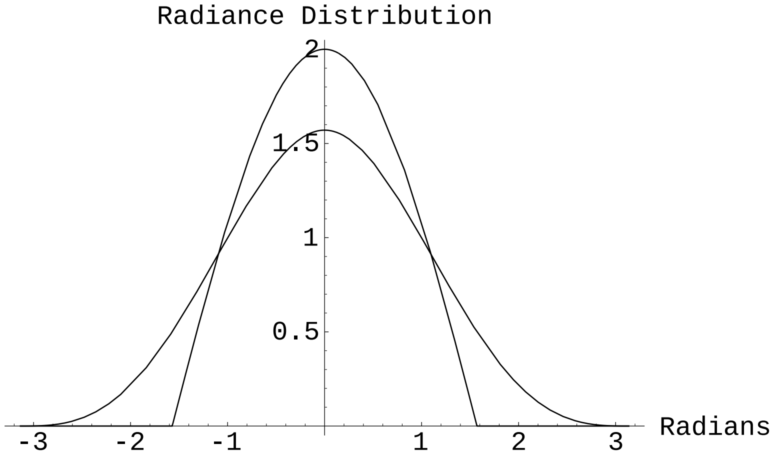

Figure 1: Radiance of a cylinder depending on the direction compared with a plane patch.

most plants and organs of plants:

a) rotational surfaces (cylinders, cones, spheres) building trunks, branches, twigs, needles, buds, fruits, and blossoms as a whole

b) bicubic patches building leaves, florets

While bicubic patches that occur in nature can be sufficiently approximated either by rotational surfaces or by plane patches, rotational surfaces themselves in general cannot be replaced by a small number of plane patches for rendering purposes. The number of patches has to be sufficiently high, otherwise the approximation of the radiance of a rotational surface would be very inaccurate as Fig. 1 shows with a cylindrical Lambertian reflector that is illuminated in the front. The cylindrical patch is compared with a plane patch of the same contour. While plane patches emphasize the directions close to the surface normal and do not radiate energy besides $\left[-\frac{\pi}{2}, \frac{\pi}{2}\right]$, with the cylindrical patch a smoother distribution of energy is achieved to all directions, even to the rear.

In general large vegetation scenes can be represented as scene graphs or CSG trees that consist essentially of rotational and plane surfaces. One can imagine that the typical diffuse light of natural scenes, like forests or grass, is partly created by the large number of rotational surfaces there. The next section gives the mathematical foundation for radiance of rotational surfaces, the following sections present particular results for special surfaces.

2 MATHEMATICAL PRINCIPLE FOR ROTATIONAL SURFACES

Let i, j, k be three patches of an outdoor scene containing plane patches as well as rotational surfaces. We want to find that part of energy that is emitted by patch k reflected by patch j incident to patch i. Let patch j be a Lambertian curved surface. Let patch i and k be plane white patches, both be normal to the ray direction. This is not really a restriction: with factors ρ and $\cos\theta$ the reflectance and the direction of the surface normal can be taken into account, and with Nusselt's analogy [Sieg 81] curved surfaces can be included, too.

The distance between patch k and patch j shall be R_1, the distance between j and i shall be R_2. Fig. 2 shows the scene consisting of patches i, j, k. The distances R_1, R_2 are large compared to the sizes of the patches, so no variation of the viewing direction has to be considered. Additionally no occlusion is assumed along the rays. For real outdoor scenes one can assume or calculate a beam attenuation coefficient κ representing occlusion and translucency [Max 97] rather than calculating shadow edges. For a practical algorithm, if occlusion has influence greater than a given bound, the surface will undergo normal subdivision processing instead of being linked. The same will occur, if proximity becomes a problem.

If we apply Lambert's law to ray 1 from patch k to j, we get the radiance at an arbitrary point in j originating from k:

$$B_{kj} = \frac{B_k A_k}{\pi R_1^2} \tag{1}$$

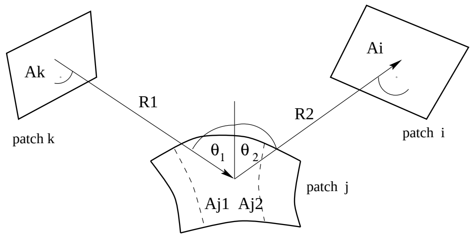

Figure 2: Curved surface illuminated by a plane patch reflecting to a plane patch.

where B_k and A_k are the radiosity and area of k respectively.

Applying Lambert's law also to ray 2 from patch j to i, we get the radiance at an arbitrary point in i reflected at j originating from k:

$$B_{kji} = \frac{\rho_j B_{kj}}{\pi R_2^2} \int\limits_{A_{j1} \cap A_{j2}} \cos\theta_1 \cos\theta_2 dA_j \qquad (2)$$

and after substitution for B_{kj}:

$$B_{kji} = \frac{\rho_j A_k B_k}{\pi^2 R_1^2 R_2^2} \int\limits_{A_{j1} \cap A_{j2}} \cos\theta_1 \cos\theta_2 dA_j \qquad (3)$$

where:

- ρ_j is the diffuse reflectance at patch j
- A_j is the area of patch j
- θ_1 is the angle between the incident ray 1 and the surface normal at a point of patch j
- θ_2 is the angle between the reflected ray 2 and the surface normal at a point of patch j
- A_{j1} is the part of patch j that is illuminated from k, that means where $cos\theta_1 \geq 0$
- A_{j2} is the part of patch j that is visible from i, that means where $cos\theta_2 \geq 0$

Therefore in (3) we integrate over the area that is visible from i as well as illuminated from k.

Up to this point no assumption was made about patch j. It could be any arbitrary curved surface. For a plane patch j $cos\theta_1$ and $cos\theta_2$ are constant because of the assumption that R_1, R_2 are large, resulting in:

$$B_{kji} = \frac{\rho_j A_j A_k B_k}{\pi^2 R_1^2 R_2^2} \cos\theta_1 \cos\theta_2 \qquad (4)$$

if i and k are visible from j, $B_{kji} = 0$ otherwise. This is the same result as if the form factors F_{jk} and F_{ij} [Cohe 85] are both applied to B_k with simplifications coming from the original assumptions about patches k and i.

If we now assume patch j to be a rotational surface, substitutions can be made for $\cos\theta_1$ and $\cos\theta_2$ because of relations in the spherical trigonometry. The $\cos\theta_l$ can also be thought as the dot product between the unity vectors in the directions of the surface normal and the incident (reflected) ray:

$$\cos\theta_1 = \sin\delta_1 \sin\alpha + \cos\delta_1 \cos\alpha \cos\varphi_1 \qquad (5)$$

$$\cos\theta_2 = \sin\delta_2 \sin\alpha + \cos\delta_2 \cos\alpha \cos\varphi_2 \qquad (6)$$

where:

- α is the angle between the tangential plane of surface j at the arbitrary point and the axis of rotation
- δ_1, δ_2 are the elevation angles of the incident and the reflected ray above the plane normal to the axis of rotation
- φ_1, φ_2 are the azimuthal angles of the rays measured from the foremost points in the directions of the incident and the reflected ray

Fig. 3 shows the relations between the angles $\alpha, \delta_1, \varphi_1, \theta_1$. The relations of $\alpha, \delta_2, \varphi_2, \theta_2$ are completely analogous. After substitution of (5) and (6) in (3) we obtain:

$$B_{kji} = \frac{\rho_j B_k A_k}{\pi^2 R_1^2 R_2^2}$$

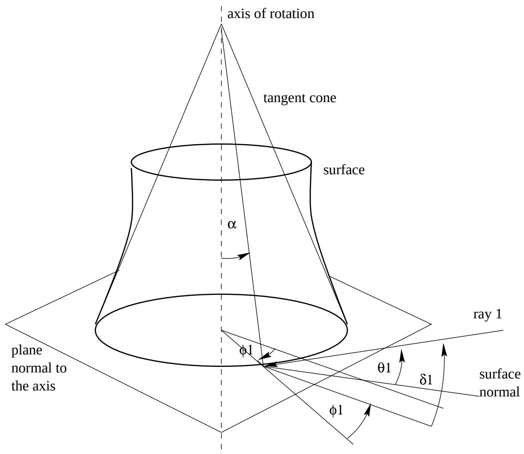

Figure 3: Angles between rotational surface and ray 1.

$$\int_{A_{j1}\cap A_{j2}} (\sin\delta_1 \sin\alpha + \cos\delta_1 \cos\alpha \cos\varphi_1) (\sin\delta_2 \sin\alpha + \cos\delta_2 \cos\alpha \cos\varphi_2) dA_j \quad (7)$$

δ_1 and δ_2 can be considered constant during integration, because of the distance assumptions. α may vary only in direction of the axis. φ_1 and φ_2 may vary only in azimuthal direction, and $\mid \varphi_1 - \varphi_2 \mid = \Phi$ is constant, it is the angle between the rays projected to the plane of rotation.

(7) seems to be no simplification for the calculation of the radiance of a rotational surface. But for special surfaces further reductions are possible.

For the cylinder:

$$\begin{aligned} \alpha &= 0 \\ \sin\alpha &= 0 \\ \cos\alpha &= 1 \end{aligned} \quad (8)$$

For the cone:

$$\alpha = \text{constant} \neq 0 \quad (9)$$

For the sphere:

because the axis of rotation can be freely chosen, it can be chosen normal to the rays so that:

$$\begin{aligned} \delta_l &= 0 \\ \sin\delta_l &= 0 \quad for \quad l = 1,2 \\ \cos\delta_l &= 1 \end{aligned} \quad (10)$$

In the following sections calculations for these special surfaces are given.

Another special case is $\alpha = \frac{\pi}{2}, \sin\alpha = 1, \cos\alpha = 0$ giving the radiance of a plane disk patch [Wall 89].

3 RADIANCE OF CYLINDERS

With the definitions of (8) we can calculate the radiance at patch i originating from a patch k reflected at a Lambertian surface j that has the shape of a cylinder. Fig. 4 shows a cylinder that is a Lambertian surface with the incident and reflected rays. $\varphi_1 = \Phi + \varphi_2$ can be assumed without restriction. Since

$$dA_j = r d\varphi_2 dh \quad (11)$$

(7) with the substitutions of (8) can be expressed as

$$B_{kji} = \frac{\rho_j A_k B_k}{\pi^2 R_1^2 R_2^2} \int_0^H \int_{-\frac{\pi}{2}}^{\frac{\pi}{2}-\Phi} \cos(\Phi + \varphi_2) \cos\varphi_2 \cos\delta_1 \cos\delta_2 r d\varphi_2 dh \quad (12)$$

and the definite integrals can be solved:

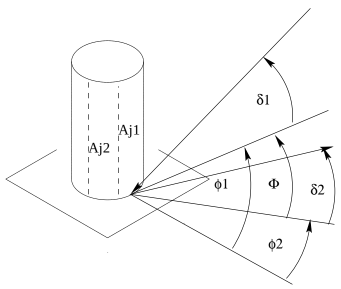

Figure 4: Cylinder with incident and reflected rays.

$$B_{kji} = \frac{\rho_j A_k B_k}{\pi^2 R_1^2 R_2^2} r H \cos\delta_1 \cos\delta_2 \left[\frac{\pi - \Phi}{2}\cos\Phi + \frac{1}{2}\sin\Phi\right] \quad (13)$$

where:

- r is the radius of the cylinder
- H is the height of the cylinder
- $\Phi = \mid \varphi_1 - \varphi_2 \mid$ is the positive angle between the incident ray and the reflected ray projected to the normal plane
- δ_1, δ_2 are the elevation angles of the rays above the normal plane

It should be noted that the result shows the typical cylinder–isotropical properties, that means it depends only on the elevation δ_1, δ_2 and the difference $\mid \varphi_1 - \varphi_2 \mid$. If $\Phi = 0$ is set in (13) then the energy reflected in the opposite direction of the incident ray is calculated. The term in the brackets becomes $\frac{\pi}{2}$. That means the energy reflected off of a cylinder is $\frac{\pi}{4}$ times or 79 % of the energy reflected by a plane patch of the same contour.

4 RADIANCE OF CONES

For cones or truncated cones one has to use (7) in full generality with α constant. In this form the definite integral is practically not computable. So we have to make some assumptions for simplification:

— the angles $\alpha, \delta_1, \delta_2$ should be close to 0, so the trigonometric functions sine and tangent can be replaced by the argument at some places. For practical computation the angles should be in the interval $\left[-\frac{\pi}{4}, \frac{\pi}{4}\right]$ for that simplification.

— the sets A_{j1} and A_{j2} are each maybe larger than the half cone but smaller than the full cone. They have an intersection that is one set, and neither contains the other (In some extreme cases two intersection sets are possible!).

The above assumptions are not too restricting, they only imply true frontal views of the cone by the patches i and k. Fig. 5 shows the frustrum of a cone that is a Lambertian surface with the above properties together with the incident and reflected rays. With these assumptions the definite integral in (7) can be approximately calculated, giving:

$$B_{kji} = \frac{\rho_j A_k B_k}{\pi^2 R_1^2 R_2^2} \int_{h_1}^{h_2} \int_{\cos\theta_1 \geq 0, \cos\theta_2 \geq 0} \frac{\cos\theta_1 \cos\theta_2}{\cos\alpha} h \tan\alpha \, d\varphi dh \quad (14)$$

and after integration with the approximation of $\cos\theta_i = C_i \cos\varphi_i$ for some C_i:

$$B_{kji} = \frac{\rho_j A_k B_k}{\pi^2 R_1^2 R_2^2} \frac{(r_1 + r_2)s}{2} \cos(\alpha - \delta_1)\cos(\alpha - \delta_2) \left[1 + \frac{\alpha(\delta_1 + \delta_2)}{\pi - \Phi}\right] \left[\frac{\pi - \Phi}{2}\cos\Phi + \frac{1}{2}\sin\Phi\right] \quad (15)$$

where:

- r_1, r_2 are the upper and lower radii of the cone (frustrum)

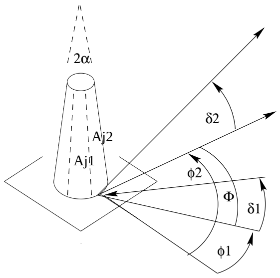

Figure 5: Cone with incident and reflected rays.

h_1, h_2 are the distances of the upper and the lower circles of the frustrum from the (virtual) top of the cone

s is the lateral line of the frustrum (of the cone)

α is the half opening angle of the cone

δ_1, δ_2 are the elevation angles of the incident and the reflected ray

Φ $=\mid \varphi_1 - \varphi_2 \mid$ is the difference of the azimuthal angles

All angles may be positive or negative. For $\alpha = 0$ (15) becomes the formula for the cylinder (13). There are three additional multiplicative terms for the cone:

$\cos(\alpha-\delta_1), \cos(\alpha-\delta_2)$ account for the changed incident and reflected angle.

$\left[1+\frac{\alpha(\delta_1+\delta_2)}{\pi-\Phi}\right]$ accounts for the shadow/visibility boundary sliding to the rear.

For $\delta_1, \delta_2 = 0$ (exact frontal view and frontal visibility) it turns out that (15) is the accurate solution without approximation.

If the cone is illuminated and visible from the top, that means there is no shadow/visibility boundary at all, then this is the special case that $A_{j1} = A_{j2} = A_j$ is the whole surface. The integration boundaries are $-\pi, \pi$, and the result can be given analytically without additonal assumptions:

$$B_{kji} = \frac{\rho_j A_k B_k}{\pi R_1^2 R_2^2} \frac{(r_1 + r_2)s}{2}$$

$$\left[2 \sin\delta_1 \sin\delta_2 (\sin\alpha)^2 + \cos\delta_1 \cos\delta_2 (\cos\alpha)^2 \cos\Phi\right] \tag{16}$$

with the same meanings of the symbols as in (15).

5 RADIANCE OF SPHERES

For spheres because of their spherical symmetry, $\delta_1, \delta_2 = 0$ can be assumed without restriction. α may vary between $-\frac{\pi}{2}$ and $\frac{\pi}{2}$ during integration. That means the axis of rotation is determined by the incident and the reflected ray to be normal to both. Fig. 6 shows a sphere that is a Lambertian surface together with the incident and reflected rays.

The integration can be thought to run over small frustra of cones from one pole of the sphere to the other. For this purpose only the special case for the cone is used with $\delta_1 = 0$ and $\delta_2 = 0$. In this case (15) is the accurate solution for the cone. The radiance of the sphere becomes:

$$B_{kji} = \frac{\rho_j A_k B_k}{\pi^2 R_1^2 R_2^2} \frac{4r^2}{3} \left[\frac{\pi - \Phi}{2} \cos\Phi + \frac{1}{2} \sin\Phi\right] \tag{17}$$

where:

r is the radius of the sphere

Φ $=\mid \varphi_1 - \varphi_2 \mid$ is the angle between the incident and the reflected ray.

For $\Phi = 0$ we receive the radiance of the full moon:

$$B_{kji} = \frac{\rho_j A_k B_k}{\pi^2 R_1^2 R_2^2} \frac{2r^2\pi}{3} \tag{18}$$

Compared with a disk of the same size the radiance of the full moon is only 2/3 or 67 %.

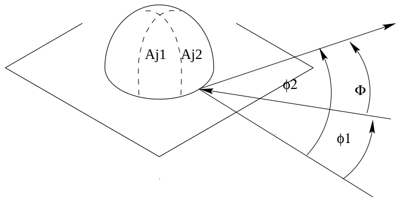

Figure 6: Sphere with incident and reflected rays.

6 FUTURE PLANS FOR A COMMON RADIOSITY ALGORITHM

If more general surfaces than cylinders, cones and spheres shall be rendered, one can either try to solve the integrals (3) or (7) analytically or one can partition a rotational surface into finite and/or infinite frustra of cones. The first approach will in most cases lead to very complicated and unwieldy mathematical expressions.

The second approach will normally work, if selfocclusion of the parts can be estimated realistically, e. g. for a sequence of branches of a tree, or selfocclusion is impossible because of the convex shape of the surface, e. g. an ellipsoid or a paraboloid.

Clusters of particles have been investigated [Sill 95] concerning occlusion, translucency and attenuation of light. Not too much investigation was done on the diffuse reflection of clusters. But there are many parallelisms and analogies between rotational surfaces and clusters of particles. They have not been studied in detail up to now. Since clusters of particles are very important for the rendering of vegetation scenes, clusters should be handled in a similar way as rotational surfaces are, if the stochastic properties of the clusters are sufficiently symmetric (either cylindrical or spherical).

For the three simplest rotational surfaces it could be shown, that their radiance is mathematically expressable and computable. Cylinders, cones and spheres are heavily used for modelling plants mathematically for the purpose of graphical rendering. The next step will be to study the interactions of light between surfaces and clusters of particles. Finally a common radiosity algorithm should be developed that comprises plane patches, curved surfaces and clusters.

In section 2 formula (2) shows that the radiance B_{kji} at a patch i originating from k reflected at a curved surface j can be expressed in B_{kj}, the radiance at j coming from k. That relation suggests a three point clustering algorithm in a line space hierarchy as described in [Dret 97] and in [Stam 98] to be used as the basic algorithm. The subdivision oracle has to be modified in the sense that the energy transfer has to be calculated analytically for rotational objects whenever possible rather than subdividing the objects.

REFERENCES

[Cohe 85] M. Cohen, D. Greenberg: The Hemi-Cube – A Radiosity Solution for Complex Environments. *Computer Graphics*, 19(3), 1985

[Cohe 86] M. Cohen, D. Greenberg, D. Immel, P. Brock: An Efficient Radiosity Approach for Realistic Image Synthesis. *IEEE Computer Graphics and Applications*, 6(2), 1986

[Cohe 88] M. Cohen, S. Chen, J. Wallace, D. Greenberg: A Progressive Refinement Approach for Fast Radiosity Image Generation. *Computer Graphics*, 22(4), 1988

[Dret 97] G. Drettakis and F. Sillion: Interactive Update of Global Illumination using a Line–Space Hierarchy. *Computer Graphics (SIGGRAPH '97Proceedings)*, August 1997

[Gerv 96] M. Gervautz, C. Traxler: Representation and Realistic Rendering of Natural Phenomena with Cyclic CSG Graphs. *The Visual Computer*, 12, Springer, 1996

[Gora 84] C. Goral, K. Torrance, D. Greenberg, B. Battaille: Modelling the Interaction of Light Between Diffuse Surfaces. *Computer Graphics*, 18(3), 1984

[Hanr 91] P. Hanrahan, D. Salzmann, L. Aupperle: A Rapid Hierarchical Radiosity Algorithm. *Computer Graphics*, 25(4), 1991

[Max 97] N. Max, C. Mobley, B. Keating, En-Hua Wu: Plane–Parallel Radiance Transport for Global Illumination in Vegetation. *Rendering Techniques '97 (Proceedings of the 8th Eurographics Workshop on Rendering)*, St. Etienne, France, Springer, 1997

[Prus 90] P. Prusinkiewicz, A. Lindenmayer: The Algorithmic Beauty of Plants. Springer, New York, 1990. With J. S. Hanan, F. D. Fraccia, D. R. Fowler, M. J. M. de Boer, and L. Mercer.

[Shir 91] P. Shirley: Radiosity via Ray Tracing. *Graphics Gems II* (Editor: J. Arvo), Academic Press, London, 1991

[Sieg 81] R. Siegel, J. Howell: Thermal Radiation Heat Transfer. *McGraw-Hill*, New York, 1981

[Sill 95] F. Sillion, G. Drettakis, C. Soler: A Clustering Algorithm for Radiance Calculation in General Environments. *Rendering Techniques '95 (Proceedings of the 6th Eurographics Workshop on Rendering)*, Dublin, Ireland, Springer, 1995

[Stam 97] M. Stamminger, P. Slusallek, H. Seidel: Bounded Radiosity – Illumination on General Surfaces and Clusters. *Computer Graphics Forum (EUROGRAPHICS '97 Proceedings)*, 16(3), September 1997

[Stam 98] M. Stamminger, P. Slusallek, H. Seidel: Three Point Clustering for Radiance Computations. *Rendering Techniques '98 (Proceedings of the 9th Eurographics Workshop on Rendering)*, Vienna, Austria, Springer 1997

[Wall 89] J. Wallace, K. Elmquist, E. Haines: A Ray Tracing Algorithm forProgressive Radiosity. *Computer Graphics Proceedings*, Boston, 1989

[Zatz 93] H. Zatz: Galerkin Radiosity: A Higher Order Solution Method for Global Illumination. *Computer Graphics Proceedings*, 1993